

**GROWTH AND CHARACTERIZATION  
OF ZINC OXIDE NANOSTRUCTURES  
BY  
LOCAL HEATING METHOD**

Dissertation submitted in partial fulfilment of the requirements for the degree of

**MASTER OF SCIENCE  
IN  
PHYSICS**

By

**Shubhra Dash**

**Roll no 412PH2093**



**Under the Supervision  
Of**

**Dr. Jyoti Prakash Kar**

**DEPARTMENT OF PHYSICS  
NATIONAL INSTITUTE OF TECHNOLOGY,  
ROURKELA  
ODISHA-769008  
2012-2014**

**Department of Physics**  
**National Institute of Technology, Rourkela**



**CERTIFICATE**

This is to certify that the work in the report entitled “**GROWTH AND CHARACTERIZATION OF ZINC OXIDE NANOSTRUCTURES BY LOCAL HEATING METHOD**” by Shubhra Dash, in partial fulfilment of Master of Science degree in PHYSICS at National Institute of Technology, Rourkela, is an authentic work carried out by her under my supervision and guidance. The work is satisfactory to the best of my knowledge.

Date- 10-05-2014

Place- Rourkela

**Dr. Jyoti Prakash Kar**

Assistant Professor

Department of Physics

National Institute of Technology, Rourkela

## ACKNOWLEDGEMENT

First and foremost I would like to express my sincere thanks and deepest gratitude to my supervisor **Dr. Jyoti Prakash Kar**, Department Of Physics NIT Rourkela, for his constant motivation, inspiration and caring support during the course of my project work. I truly appreciate his guidance and encouragement from the beginning to the end of this project work without which the project would not have been possible.

I also wish to express my sincere thanks to our research scholars **Mr. Surya Prakash Ghosh, Mr. Kailash Chandra Das** and **Mr. Nilakantha Tripathy** for giving me attention and time. Their continuous encouragement, co-operation, caring and valuable guidance helped me a lot to carry out my project work successfully.

I express my sincere thanks to all the faculty members of Department of Physics, NIT Rourkela who have made direct or indirect contribution towards the completion of this project. I also thank all my friends and all the lab members of the Dept. of Physics for their helping hands which leads to the successful completion of my project. Last but not the least, I would like to record deep respect to my parents for selflessly extending their ceaseless support.

10-5-2014

Shubhra Dash

# CONTENTS

ACKNOWLEDGEMENT

LIST OF FIGURES

ABSTRACT

CHAPTER-1

Introduction .....	1
1.1 .Zinc Oxide Structure and Properties.....	2
1.2 .Thin Films.....	3
1.3 .1D Nanostructures and Their Importance.....	4
1.4 .Growth Methods of Zinc Oxide 1D Nanostructures.....	5
1.4.1. Parameters for 1D nanostructures growth.....	6

CHAPTER-2

Literature Survey.....	8
------------------------	---

CHAPTER-3

Experimental Methodology.....	10
3.1.Deposition of ZnO thin film on Silicon substrate by RF Sputtering.....	10
3.1.1.Choice of substrate.....	10
3.1.2.Substrate Cleaning.....	10
3.1.3.ZnO thin film deposition.....	10
3.2 .1D ZnO Nanostructures growth.....	12
3.2.1. Local heating Method.....	12
3.3. Surface Functionalization with Poly Styrene Sulfonate (PSS).....	13

## **CHAPTER-4**

<b>Characterization Techniques .....</b>	<b>14</b>
<b>4.1. X-Ray Diffraction.....</b>	<b>14</b>
<b>4.2. Field Emission Scanning Electron Microscope (FESEM).....</b>	<b>15</b>
<b>4.3. Fourier Transformed Infrared Spectroscopy (FTIR).....</b>	<b>16</b>
<b>4.4. Current Voltage (I-V) Measurement.....</b>	<b>17</b>
<b>4.5. UV Detection.....</b>	<b>17</b>

## **CHAPTER-5**

<b>Results and discussion.....</b>	<b>19</b>
<b>5.1. X-Ray Diffraction.....</b>	<b>19</b>
<b>5.2. Field Emission Scanning Electron Microscope (FESEM).....</b>	<b>20</b>
<b>5.3. Fourier Transformed Infrared Spectroscopy (FTIR).....</b>	<b>21</b>
<b>5.4. Current Voltage (I-V) Measurement.....</b>	<b>22</b>
<b>5.5. UV Detection.....</b>	<b>22</b>

## **CHAPTER-6**

<b>Conclusion.....</b>	<b>24</b>
<b>REFERENCES.....</b>	<b>25</b>

## LIST OF FIGURES

Figure.1.1. Zinc interstitial sites in the ZnO wurtzite lattice.....	2
Figure.1.2.1.Deposition Mechanism of Thin Films.....	4
Fig.3.1.3.1.Schematic diagram of RF sputtering.....	11
Fig.4.1.1. Bragg's Law.....	14
Fig.4.3.1.Schematic diagram of Fourier Transform Infrared Spectroscopy.....	16
Fig.4.4.1.Keithley 6487Picoammeter.....	17
Figure 5.1.1.(a, b) XRD pattern of ZnO Nanostructures synthesised at different temperature and concentration.....	19
Figure.5.2.1. (a, b, c) FE-SEM images of the 1D ZnO nanostructures synthesized in aqueous solution with various molar concentration and temperature.....	20
Figure.5.3.1. (a,b) FTIR spectra of ZnO nanostructures synthesized at different concentrations.....	21
Figure.5.4.1. I-V characteristics of ZnO/Si nanorod before and after UV illumination of (a)Uncoated (b)PSSCoated.....	22
Figure.5.5.1. Time evolved photo response of nanorods with PSS coating and without coating.....	23

## Abstract

In the present work 1D Zinc Oxide nanostructures were synthesized successfully by local heating method at various concentration and temperature. Crystalline nature of ZnO nanostructures was confirmed by the appearance of high intensity peak at (0 0 2) in X-ray diffraction analysis of different samples. FESEM analysis confirmed the formation of long 1D ZnO nanostructures of about 4.5 $\mu$ m in length. The effective synthesis of ZnO nanostructures from the oxidation of Zn was also confirmed by FTIR analyses. The UV detection characteristics of the ZnO/Si nanostructures were studied by measuring current-voltage I-V relationships with and without UV-B light (310-370) nm. UV detection was studied and shows the time evolution of current of the nanorods under UV illumination for surface with modification by coating Poly Styrene Sulfonate (PSS).

**Keywords:** Zinc oxide, nanostructures, RF sputtering, local heating, UV detection

# CHAPTER- 1

## Introduction

Semiconducting materials played a vital role in the growth of our technical civilization over the last six decades. In comparison with Si and Ge, ZnO, the compound semiconductor has the advantage of direct wide band gap, which allows operation of devices at higher temperatures, and gives lower thermal noise to low power devices at room temperature and favourable for short wavelength optoelectronic properties. ZnO also shows much advantage when compared with its main competitor GaN. As like GaN, ZnO also crystallizes in the wurtzite structure but in contrast, ZnO is a n-type semiconductor and available as large bulk a single crystal which is a vital advantage of ZnO over GaN [1]. ZnO exhibits exceptionally high radiation hardness than Si, GaAs, CdS and that of GaN making it suitable for the applications at high altitude or in space [2]. The band gap of ZnO is 3.44 eV at low temperatures and 3.37 eV at room temperature comparable to wurtzite GaN that is 3.50 eV and 3.44 eV, which enables applications in optoelectronics [3] in the blue/UV region, including light-emitting diodes, laser diodes and photo detectors [2]. ZnO possesses a large binding energy of 60 meV which makes it a suitable candidate for giving higher UV emitting frequency at room temperature [4]. Higher exciton binding energy of ZnO is the key factor to show a better optoelectronic property [6]. Another advantage over GaN is that ZnO is responsive to wet chemical etching which is helpful in device fabrication. Due to the high electron mobility, high thermal conductivity, high heat capacity, low melting temperature and low thermal expansion ZnO is a step ahead than those of the traditional semiconductors.

### 1.1. Zinc Oxide Structure and Properties

ZnO is an II-VI group compound semiconductor due to the fact that Zn belongs to II group and O belongs to VI group. ZnO shows ionic nature which is in between covalent and ionic semiconductor. ZnO can form crystal structures like Wurtzite, Zincblende, and rock salt but the wurtzite phase is generally stable at room temperature. ZnO has a hexagonal unit cell with a  $c/a$  ratio of 1.633 and it belongs to the space group of  $P6_3mc$  [8]. Two interconnecting sublattices of Zn and O form the hexagonal lattice of ZnO.

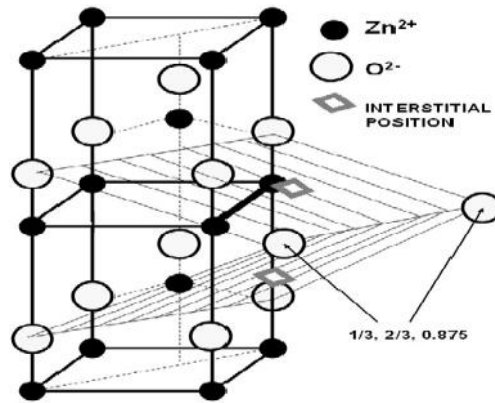


Figure.1.1.ZnO Crystal structure [7]

Table .1.1.Properties of Zinc Oxide [5]

<b>Crystal Structure</b>	<b>Hexagonal, Wurtzite</b>
<b>Lattice constant</b>	<b>a = 3.246 Å, c = 5.207 Å</b>
<b>Cohesive energy</b>	<b>1.89 eV</b>
<b>Electron mobility</b>	<b>100 cm<sup>2</sup>/vs</b>
<b>Exciton binding energy</b>	<b>60 meV</b>
<b>Band gap at RT</b>	<b>3.37 eV(direct)</b>
<b>Density</b>	<b>5.67 g/cm<sup>3</sup></b>
<b>Molecular weight</b>	<b>81.38 g/mol</b>
<b>Melting point</b>	<b>1975<sup>0</sup>C</b>
<b>Refractive Index</b>	<b>2.00</b>
<b>Specific heat</b>	<b>40.3 J mol<sup>-1</sup>K<sup>-1</sup></b>
<b>Thermal conductivity</b>	<b>(.6-1)W cm<sup>-1</sup>K<sup>-1</sup></b>

## 1.2. Thin Films

Thin films have many interesting properties which differ from their bulk counterpart due to the increase of surface to volume ratio. The first observation and interpretation for thin film was by R.Boyle, Hooke and Newton in the year 1650 by considering the interference pattern of oil on water while the development of deposition techniques was first done in 1850[9]. Later in 1965 thin film technology takes an integral part in the semiconductor industry. The tuning of material properties to the atomic dimensions with the fabrication of different microstructures was found to have increasing interest after 1995[9].

For thin film deposition a thick supporting base material is needed to hold the film known as the substrate. Generally, the substrate thickness is from few micrometer to millimetre range where as the thickness of the film varies from few angstroms to micrometer[10]. An ideal thin film is a two dimensional object which has the extension in two direction while restriction is in the other direction. Nature and properties of the film depends upon the growth conditions. Thin films are grown by impinging atoms onto the substrate surface by changing the experimental conditions which can affect the film quality.

Ideally, in the thin film deposition process involves atom by atom deposition with a sufficient time interval between the successive deposition of atoms or layers in order to have a minimum potential which is thermodynamically stable [10]. Thus in a thermodynamically stable film all the atoms and the molecules are in their minimum energy state and the incoming atoms occupy positions and orientations compatible to the neighbouring atoms or the previously deposited layer. Any deviations from the ideal conditions lead to the formation of metastable film.



Figure.1.2.1.Deposition Mechanism of Thin Films

### 1.3. 1D Nanostructures and Their Importance

Nanostructures and nanomaterials are a matter of research focus due to their unique features and vast applications in various fields. It is the large surface to volume ratio (aspect ratio) of nanomaterials which contribute to the better thermodynamic properties. The size of the nanoparticles is comparable to the exciton Bohr radius which greatly changes the optical, luminescent and redox properties.

Large aspect ratio and the trap centres found in semiconducting 1D ZnO nanostructures are the main reason for getting advantage over other type of nanostructures. Due to the multifunctional properties of Zinc oxide, it creates much attention in the research field related to various applications. By applying wide number of synthesis techniques different 1D ZnO nanostructures with different shapes ranging from nanowires to nanobelts can be synthesized. The large exciton binding energy makes ZnO an eligible candidate to persist at room temperature and higher also [5]. This property helps to fabricate many fine optical devices using ZnO nanostructures.

1D nanostructures such as nanowires and nanorods have dimension of 1-100 nm and are attributed to the class of nanocrystalline materials due to the elongation in only one direction. Various ligands act as shape controlling agent for the nanorods when bonded to different facets which allows growing nanorods from initial nuclei making it an elongated species [11]. Due to the unique and variety of nanostructures achieved, ZnO is known to be the fundamental material in structure and property.

#### 1.4. Growth Methods of 1 D Zinc Oxide Nanostructures

1D ZnO nanostructures with different morphology can be grown by Physical vapour deposition [12], Metal–Organic Chemical Vapour Deposition (MOCVD) [13], Molecular Beam Epitaxy (MBE) [14], hydrothermal/solvothermal methods [14, 15] and top down approach [16]. ZnO nanostructures can mainly be synthesized by both vapour phase synthesis and solution phase synthesis.

Among the vapour phase synthesis Vapour Liquid Solid (VLS) has the advantage that it can grow ZnO on large substrates. But it requires a high temperature of 500°C-1500°C and the use of metal catalysts causes contamination to the product formed [18]. MOCVD and MBE can give high quality ZnO nanorod arrays, but use the high cost equipment, low output and limited choices of substrate makes it complicated for large scale production [17, 19]. Another simple and low temperature method is the Physical Vapour Deposition (PVD) by which we can get pure ZnO nanowires with high crystal quality [20].

But the solution phase synthesis has much advantage in comparison to vapour phase synthesis due to the low temperature process (<200°C), low cost and handy [21]. Both organic and inorganic substrates can be used in case of hydrothermal method which has much advantages when compared to other growth methods [21]. 1D nanostructures can be prepared more easily by hydrothermal method since it can provide the use of wide variety of precursors [20]. In aqueous growth process the reaction can be performed in aqueous or organic solution [22,23]. Solution-based methods offer several advantages such as use of wide variety of precursors, environmental friendliness and simplicity compared to top-down-based methods like lithography. Organic synthesis from chemical solutions include precipitation, sol–gel-based methods, hydrothermal synthesis, combustion synthesis, molten salt method and spray pyrolysis among others [20,21]. Hydrothermal synthesis involves heating the chemical solution in a sealed vessel. If water is used as the solvent, the process is called hydrothermal while when any non-aqueous solvent is used as solvent then the process is said to be solvothermal [24].

Water is environmental friendly and thus can be used as a preferred solvent. Due to this hydrothermal methods have received a lot of attention and have been widely used for synthesis of 1D nanomaterial. Due to the oxygen vacancy ZnO nanostructures grown by hydrothermal method show crystalline defects and are thus capable of various applications [21]. In addition, hydrothermally grown ZnO nanowires are capable of exhibiting visible light

photo catalysis even without doping with transition metals [25]. Large scale growth of aligned ZnO nanowires with high aspect ratio on arbitrary substrates can be obtained by hydrothermal method. This method provides numerous advantages due to the simple, low temperature growth and no uses of metal catalyst [26]. Low temperature aqueous solution growth of ZnO nanostructures provides the fabrication of nanostructures with controlled preferential orientation along the C-axis and crystalline morphology. The ZnO nanostructures obtained by this method has low defect concentration which is helpful in sharp emission with increase in intensity [26]. 1D ZnO nanostructures obtained by hydrothermal method provide enormous advantages such as high aspect ratio, good field electron emission property and excellent molecular absorption and desorption characteristics in catalyst applications [27].

The morphology of the 1D ZnO nanostructures greatly depends upon the thickness of the seed layer and the seed layer provides better adhesion to the nanowires [28]. Use of ZnO film as an intermediate layer on the substrate helps to get vertically aligned ZnO nanowires [29]. Various techniques have been employed to prepare ZnO films such as sol-gel process, chemical vapour deposition, pulsed laser deposition, direct current (DC) and radio frequency (RF) sputtering. The RF sputtering technique has drawn considerable attention due to its reproducibility. Thus for growing the seed layer on the substrate radio frequency (RF) sputtering deposition technique is a better option in order to have a C-axis oriented ZnO film with high quality and better crystallinity [30].

#### **1.4.1. Parameters for 1D nanostructures growth**

Various parameters which affect the growth of 1D nanostructures are

- **Degree of supersaturation of reactants:**  
Because of the formation of critical nuclei, high supersaturation level promotes the nucleation process where as low saturation favours the crystal growth [21].
- **Effect of seeding layer:**  
By growing a seed layer on the substrate the adhesion property of the nanostructure to the substrate can be enhanced which leads for the formation of vertically aligned 1 D nanostructure [21].
- **Effect of precursor concentration:**  
Precursor concentration determines the nanostructure density. By increasing the precursor concentration the average diameter of the 1D nanostructure will increase but

however the changes in the concentration ratio of the reactant have no significant effect on the diameter of the 1D nanostructure [21].

- **Effect of growth temperature:**

Growth temperature and time controls the nanostructure morphology and aspect ratio. Growth temperature depends on the amount of reactive vapour generated and the surface diffusion length of the adsorbed species. Surface diffusion and condensation of vapour affects the growth rate [21].

For the growth of 1D nanostructures always low temperature is favourable because at high temperature, the growth species get enough energy to diffuse and can attain their favourable minimum energy state. But the high thermal energy also causes a high rate of adsorption and re evaporation which leads to dense and short nanostructures.

At low temperature the reactant vapour atoms has much low energy and is not sufficient for the atoms to diffuse as a result the atoms just come and sit at the positions where they land creating a rough uneven film of the nuclei clusters and thus leads to the formation of several nanostructures.

In conventional hydrothermal method where global heating of the precursor solution takes place limits the length of the 1D nano structures to only 2-3 $\mu$ m due to the precursor consumption[31]. So here a better approach has been tried to get long 1D nanostructures by local heating method, where the precursor solution is not preheated rather the substrate is heated only at particular points to supply fresh precursors.

## CHAPTER- 2

### Literature Survey

1D ZnO nanostructures are of increasing interest due to their applications in various areas due to their electronic and optoelectronic properties. For this they can be used in UV light emitting diodes, UV photo detectors, solar cells, UV nano laser, field effect transistors etc. By applying different growth methods various 1D ZnO nanostructures with different morphology can be developed [13]. Surface of the nanostructures plays an important role in determining the optoelectronic properties of nano-devices due to their large surface to volume ratio. Due to this unique property the nanoscale electronic devices can achieve higher sensitivity and faster response than the bulk material [13]. It was Kind et al. who have reported for the first time the effect of UV photo detection from single ZnO nanostructures. Many efforts have been made to improve the detection of photon and the corresponding response behaviour of the 1D ZnO nanostructures including nanowires and nanorods. It is known that, light detection and response of the ZnO nanorods depends on the synthesis methods, surface condition, morphology and rate of oxygen adsorption-desorption [32].

J. Kim and I. Park have grown ZnO nanostructures on silicon chips on a seed layer within PDMS micro channel by hydrothermal method [33]. They have tried in different ways to grow the nanostructures by globally as well locally by taking zinc nitrate, hexamethylene tetra amine and polyethyleneimine as the precursors. They have supplied the fresh precursor solution to the micro channel by syringe pumps. For global synthesis the precursor solution was preheated and for the local synthesis thermal energy was supplied to the micro heater while solution was flowing through the channel. They have found that nanostructures grown by localized heating were much vertically aligned.

Jung Kim et al have synthesized ZnO 1D nanostructures by either on the entire substrate or on the patterned area along the micro heaters within the microfluidic channel and they have found that 1D nanostructures grown only on the micro heaters are much vertically aligned due to the localized endothermic reaction [34]. Zheng J. Chew and Lijie Li have employed localized growth of ZnO 1D nanostructures by Joule heating on a printed circuit board [35]. For the synthesis of ZnO 1D nanostructures they have used a seed layer made of zinc acetate dihydrate in DI water. Joule heating was carried out by passing current to the conducting track so that zinc acetate dihydrate decomposed to form zinc oxide nano crystals

and after that they have carried out a hydrothermal synthesis of the ZnO 1D nanostructures. They have found that dense ZnO 1D nanostructures were grown on the central part of the heated zone.

D. Kim et al. have fabricated ZnO 1D nanostructures based gas sensing device where the 1D nanostructures were grown by localized heating by utilizing the localized thermal energy given by the micro heater arrays integrated in the device [36]. It has been revealed that the micro heaters below the sensing electrodes supply localized heating to initiate a selective and direct growth of ZnO NWs between the electrodes. For the ZnO 1D nanostructures growth they have used aqueous solution of Zinc nitrate, HMTA and PEI as the precursor and were put onto the PDMS block over the chip [36]. A micro heater array to the solution was connected to heat the solution to about 95°C for the synthesis of 1D nanostructures. C.C. Chen et al have reported a mask free technique for the local synthesis of ZnO 1D nanostructures on Poly silicon nanobelts and poly silicon 1D nanostructures device. In order to get ZnO 1D nanostructures selectively in the localized Joule heating region they have done the selective patterning of the seed layer. It has been reported that gold nanoparticles as catalyst to initiate the growth of ZnO 1D nanostructures [37].

Lulu Chen et al have synthesized ZnO 1D nanostructures for dye sensitized solar cell applications [38]. The ZnO 1D nanostructures were synthesized by ammonium assisted hydrothermal method on the seeded FTO substrate by using zinc nitrate, ammonium hydroxide and HMTA. By changing the amount of ammonium hydroxide in the growth solution the length of the ZnO 1D nanostructures can be changed [38]. Liang-Yih Chen and Yu-Tung Yin have synthesized high crystal quality long ZnO 1D nanostructures with by Continuous Flow injection process allowing a stable supply of zinc precursor concentration. They have found that ZnO 1D nanostructures were of length 20µm at 5mM concentration of the solution which decreases with increase of the precursor concentration [39].

## **CHAPTER -3**

### **Experimental Methodology**

#### **Growth of Nanostructures by hydrothermal method**

1D ZnO nanostructures can be grown by two step method

- Deposition of seed layer on the substrate
- Growth of Nanostructures on the deposited seed layer

### **3.1. Deposition of ZnO thin film on Silicon substrate by RF Sputtering**

#### **3.1.1. Choice of Substrate**

Nature of substrate has a vital role in the growth of nanostructures. Various substrates can be taken for the growth of nanostructures as like glass, silicon or sapphire. But among these silicon is the most promising substrate for the low cost, good thermal conductivity, high crystalline quality and the availability of large size substrates [40].

#### **3.1.2. Substrate Cleaning**

The substrate was first cleaned by acetone bath under ultrasonication for 5 minutes. Then substrate was ultrasonicated in DI water followed by isopropyl alcohol (IPA) for 5 minutes each. Next it was put for the ultrasonic cleaning in DI water for 5 minutes. Then it was allowed to dip in 1:1 volume of H<sub>2</sub>SO<sub>4</sub> and H<sub>2</sub>O<sub>2</sub> for 10 minutes to remove the oxide contents and was rinsed with DI water. Then the substrate was dipped in 5 % HF solution for 1 minute and was rinsed properly with DI water. Then the substrate was dried in the spin coating unit.

#### **3.1.3. ZnO thin film deposition**

Deposition of ZnO thin film has been done by choosing Zn as the target material and Silicon is used as the substrate. The target was applied to a positive potential and the substrate was grounded. Rotary pump was switched on and the roughing valve was opened. Pirani gauge was used to read the roughing vacuum. As soon as the Pirani gauge shows a vacuum better than 0.05m.bar diffusion pump was switched on. water connections were given to the diffusion pump cooling line. The diffusion pump takes about 30 minutes to

attain the operating temperature so in the meantime, air admittance valve was opened slowly and after cleaning the chamber substrate was mounted. After loading substrates the chamber and venting valve and the backing valves were closed and the roughing valve was opened. High vacuum valve was also opened. Water supply to the heater was on during this time and the substrate was heated at 200°C after getting a vacuum of the order of  $10^{-6}$  mbar. Electrical connections of RF power supply to the target guns and the gas connections was done. Substrate rotation was provided and the chamber pressure was decreased from  $10^{-6}$  mbar to  $10^{-2}$  mbar by allowing Argon and oxygen gas to flow into the chamber by closing partially the high vacuum valve. The flow ratio of argon and oxygen was maintained at 2:3. The high vacuum valve was adjusted to achieve a constant pressure of  $9.2 \times 10^{-7}$  mbar. Water supply to the target was given and the RF power (13.56 MHz) of 150 watt was applied and the reflected power was reduced by the matching network in order to get stable plasma with shutter closed. Presputtering was carried out for 15 minutes. The working pressure was fixed at  $8 \times 10^{-3}$  mbar. During sputtering the energetic ions strike the Zn target and dislodge the target (Zn) atoms. The atoms travel freely in the plasma in the vapour state and react with the oxygen gas to form a compound ZnO film. The target shutter, substrate shutter was opened and the deposition was done for 60 minutes. After completion of deposition the RF power and the gas flow was switched off. 10 minutes was given for the cooling of the target and substrate. Water connections were stopped and the Pirani and high vacuum valve was closed. The sample was taken outside by venting the chamber.

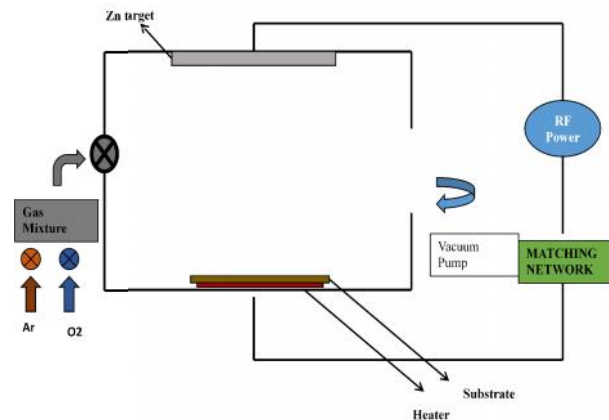


Fig.3.1.3.1. Schematic diagram of RF sputtering

**Table. 2.1. Working Parameters**

Substrate type	Silicon p-type
Distance from source to target	10cm
Base pressure	$9.2 \times 10^{-7}$ mbar
Working Pressure	$8 \times 10^{-3}$ mbar
Substrate temperature	200°C
Ar:O <sub>2</sub>	2:3
RF power	150W
Predeposition time	12min
Deposition time	30min

## 3.2. 1D ZnO Nanostructures growth

### 3.2.1. Local heating Method

This method which allows us to get uniform, homogenous, aligned long 1D nanostructures which has significant advantages than that of the conventional global heating method. In case of conventional hydrothermal method global heating of the solution takes place. Thus in the global synthesis method the precursor solution is preheated and the substrate is also heated. But in case of local synthesis precursor solution is not preheated whether only the substrate is heated at through the heater when the substrate is inside the precursor solution. Due to the restricted area heating the critical size of the nuclei get sufficient time to favours the formation of long 1D nanostructures rather than producing undesired nanostructures. Since the whole solution is not heated thus the reactants get sufficient time to form the product. By using this method one can find ultra long nanowires without the addition of any extra chemicals. This method can provide a wide platform for the fabrication of 1D nanostructures based electronic device and the various sensing materials.

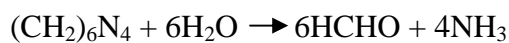
For the growth of ZnO nanowire by local heating method the precursor solutions used were zinc nitrate[  $Zn(NO_3)_2$  ] and hexamethylene tetra amine(HMTA)[  $C_6H_{12}N_4$ ]. Equimolar

concentration of zinc nitrate and HMTA was prepared in de ionized (DI) water and was mixed properly. The seed layer was put in the beaker containing the precursor solution. The beaker was placed inside a container containing water for the cooling purpose of the solution. The set up was connected to a PID controller where the time and temperature was set and the reaction was allowed to take place.

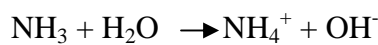
$Zn(NO_3)_2$  is a salt which provides  $Zn^{2+}$  which is required for the building up of the ZnO nanowire.  $H_2O$  molecules in the solution provides  $O^{2-}$  ions. HMTA is a non cyclic tertiary amine which acts like a bidentate Lewis base which coordinates to two  $Zn^{2+}$  ions. Attachment of HMTA to the non polar side facets helps in the anisotropic growth of 1D ZnO nanostructure in [0001] direction [41].

The reaction mechanism is as follows:

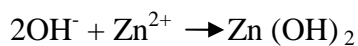
Decomposition reaction:



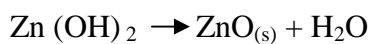
Hydroxyl supply reaction:



Supersaturation reaction:



1 D ZnO nanostructure growth reaction:



### 3.3. Surface Functionalization with Poly Styrene Sulfonate (PSS)

The surface functionalization of the nanostructures was done by first adsorbing a polymer, poly(diallyldimethylammonium chloride) PDADMAC onto its surface by electrostatic attraction force between the negative surface charges of ZnO and positive charges of PDADMAC. Then, the ZnO nanorod was immersed in an anionically charged polymer solution of Poly Styrene Sulfonate (PSS), which was adsorbed on the ZnO nanorod owing to the electrostatic force from the cationically charged PDADMAC molecules [42]. To test the UV detection metallization of the nanorod surface was done by local coating of aluminum in thermal evaporation.

## CHAPTER-4

### Characterization Techniques

#### 4.1. X-Ray Diffraction (XRD)

Physical properties of a substance depend on the arrangement of the atoms inside that so, crystal structure determination is an important part for the structural characterization of the material. When X ray passes through a material it interacts with the atoms present within it. Diffraction effect is observed when electromagnetic radiation impinges on the periodic structure with geometrical variations on length scale of wavelength of radiation. In crystals the typical interatomic spacing is about 2-3 Å for which the suitable radiation is X ray[43]. Hence X ray is used for the study of crystal structures. X ray when interacts with the atoms the electrons within the atom start vibrating with the frequency of the X ray beam and thus secondary electrons are generated and scattered in all directions. When the scattered beams are in phase then they interfere constructively meeting the criteria of Bragg's law. For defined wavelength and incident directions crystalline materials give intense peak of the scattered radiation.

Lawrence Bragg and his father W.H. Bragg discovered that diffraction can be treated as reflections from evenly spaced planes if X rays of monochromatic radiation is used and the Bragg's law can be written as  $2d\sin\theta = n\lambda$

Where  $n$  = an integer specifying order of diffraction

$\lambda$  = wavelength of X ray used

$d$  = inter planar spacing in the crystalline material

$\theta$  = diffraction angle

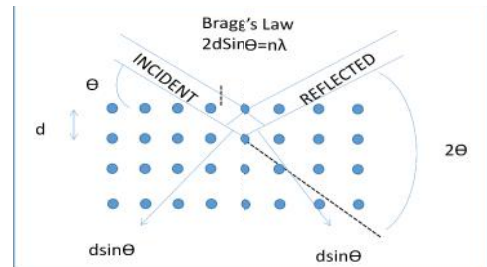


Fig.4.1.1. Bragg's Law

From the analysis of XRD pattern and comparing with the standard JCPDS reference pattern structural analysis of the specimen can be done. X Ray Diffraction also allows us to calculate the crystallite size from the Scherrer's equation given by

$$D = \frac{0.9\lambda}{\beta \cos\theta}$$

Where  $D$  = crystallite size

$\lambda$  = Wavelength of X ray

$\beta$  = Full Width at Half Maximum (FWHM)

In crystals each set of planes has specific interplanar distance and give rise to characteristic angle of diffracted X rays. When intensity vs. diffraction angle is plotted then the graph gives an idea about the number of atoms in each plane corresponding to a particular  $2\theta$  value.

From X ray diffraction we can determine

- crystallite size (Scherrer's equation)
- unit cell structure (Bravais lattice)
- Miller indices (h, k, l value)
- lattice parameter
- Types of phases present
- Crystalline or amorphous character
- Structural distortion due to unequal d spacing (strain)

## **4.2. Field Emission Scanning Electron Microscope (FESEM)**

FESEM is used to study the morphology of the specimen. In this technique, in order to get an idea about the microstructure of the sample focused electron beam is used instead of light waves. Due to the high energy of the incident electron we get quite high resolution as the wavelength gets shorter. To focus the electron beam on the sample surface electromagnetic lenses are used. FESEM can give an idea about the three dimensional information of the specimen [44].

In a typical SEM, Tungsten or Lanthanum hexaboride ( $\text{LaB}_6$ ) are used as the filament from which electrons are emitted thermionically (by giving heat to the filament) and are accelerated towards the anode, where as in case of FESEM the cathode is replaced by a field emission gun (FEG) known as the cold cathode (by giving strong electric field to the cathode to extract electron) [44]. Thermionic sources are operated below saturation for the better lifetime of the filament. FEG is best for all applications in comparison to thermo ionic gun.

Tungsten is used because of its highest melting point and lowest vapour pressure. Thus it can be heated to a high temperature to generate electrons. The electron beam, which typically has an energy ranging from a few hundred eV to 100 keV, is focused by one or two condenser lenses [44] the beam passes through pairs of scanning coils in the objective lens. Scanning coils helps in deflecting the beam horizontally and vertically which is known as raster scanning. In raster scanning each point on the sample surface is scanned serially, hence the name is scanning electron microscope[44].

When electron beam hits the specimen surface, it can penetrate up to a region known as the interaction volume. Throughout this region various radiations are generated as a result of scattering. The size of the interaction volume depends on the beam accelerating voltage, the atomic number of the specimen and the specimen's density.[44] Due to the energy exchange between the electron beam and the sample an electromagnetic radiation is emitted which is detected by the detector to produce an image.

From FESEM we can know

- surface features (Topography)
- morphology (shape and size)
- crystallographic information
- composition

### 4.3. Fourier Transforms Infrared Spectroscopy (FTIR)

The principle of FTIR is based on the fact that bonds and group of bonds vibrate at certain frequency only known as the characteristic frequency. Molecules when exposed to Infrared radiation they absorb energy at certain frequency. When nuclei of the molecules vibrate relative to each other then the internuclear distance changes and dipole moment is produced in the molecule due to difference of charges. During FTIR analysis the specimen is focused to an Infrared beam. The working principle of FTIR is based on the simple Michelson's Interferometer which works as an optical modulator and thus modulates the radiation emitted by the IR source. The transmittance and reflectance of the infrared ray at different frequencies is converted into IR absorption peak producing a broad spectrum [45].

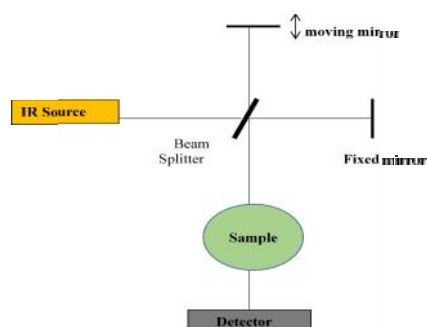


Fig.4.3.1.Schematic diagram of Fourier Transform Infrared Spectroscopy

Figure4.3.1. shows the schematic diagram of an FTIR spectroscopy which consists of a moving mirror, fixed mirror, beam splitter, IR radiation source and detector. The reflected

beam after passing through the two mirrors recombine at the beam splitter. The beam is then allowed to pass through the call and the radiation is detected by the detector.

#### **4.4. Current Voltage (I-V) Measurement**

Current Voltage measurement is a task to obtain the current vs voltage or resistance characteristics by providing a voltage/current stimulus and measuring current/voltage reaction. It is a basic electric measurement and a fundamental way to discover behaviour and characterize the devices like semiconductors and electronic devices etc.



Fig.4.4.1.Keithley 6487Picoammeter

Current voltage measurement is measured by a picoammeter by applying voltage and measuring the current.

#### **4.5. UV Detection Mechanism**

In absence of UV light the oxygen on the nanowire surface trap the free electron and is adsorbed on the surface of the nanowire. Thus there will be no more free electrons for the conduction process and as a result the conductivity will be significantly reduced with the formation of a depletion region [46].

On illumination with UV light electron holes pair are generated. Holes move to the surface of the n-type semiconducting metal oxide they discharge the adsorbed oxygen thereby decreasing the depletion region .Hence the conductivity increases. [46]

When the surface of the nanowires is illuminated with energy larger than the band gap energy than electron – hole pairs are generated. But the action of electric field holes is trapped at the semiconductor surface while the unpaired electrons are left which is the reason for increase in conductivity. [47].

Thus, in presence of UV light the current in the nanowires increases where as in absence of light it shows a decrease in the current value. The hole trapping mechanism through oxygen adsorption desorption is due to the trap centres found in the nanowires because of the unsaturated dangling bonds [47].

\

## CHAPTER -5

### Results and Discussion

#### 5.1. X-Ray Diffraction

From the figure number 5.1.1. (a) & 5.1.2. (b), shows the X-ray diffraction patterns at different temperature and concentration respectively. Diffraction pattern obtained is taken by the XRD machine model number (**Rigaku Ultima IV**) and are matched with the JCPDS file and recognized as Zinc Oxide peaks. It shows the XRD pattern of ZnO nanostructures grown on Si. Crystalline nature of ZnO nanostructures is observed with the appearance of (0 0 2) peak [48]. It shows no diffraction peaks for the impurities. The intensity of the peak is stronger along c-axis i.e. (002) which shows that ZnO nanorods are much oriented along that direction. When temperature increases growth rate of the nanorods also increases so stronger peak intensity is found with increase of temperature from 60<sup>0</sup>C to 80<sup>0</sup>C. But at the same temperature with different concentrations nearly same intensity peaks are found [48].

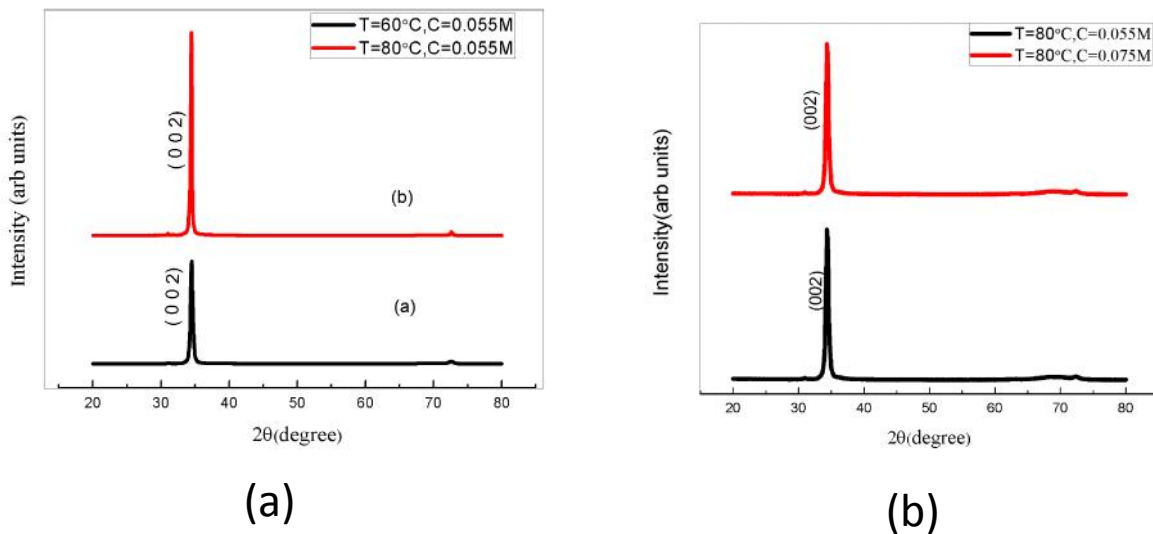


Figure 5.1.1. shows the XRD pattern of ZnO Nanostructures synthesised at different temperature and concentration. (a) XRD pattern of ZnO nanostructure synthesized at two different temperature (b) XRD pattern of ZnO nanostructures synthesized at two different concentrations 80<sup>0</sup>C.

## 5.2. Field Emission Scanning Electron Microscope (FESEM)

Figure 5.2.1. (a, b, c) illustrates the cross-sectional view of FE-SEM images of ZnO nanorods fabricated at various concentrations and different temperature of aqueous solution. Figure 5.2(a) shows the ZnO nanostructures grown at 60°C in aqueous solution having concentration of 0.055M. Since the temperature is not sufficient to complete the chemical reaction therefore 1D ZnO nanostructures are not obtained completely. As the growth temperature increases to 80°C figure.5.2.1. (c) long dense rod like nanostructures having length of about 4.5µm and diameter of about 500nm is obtained. It can be observed that concentration of aqueous solutions plays a crucial role in the synthesis of the 1D nanostructure. The FE-SEM images Figure5.2.1. (a, b) reveal that morphologies of the 1D ZnO nanostructures synthesized by various solution concentrations are apparently different. On dependence with the concentration of aqueous solution, the density of the nanostructures increases with an increase of solution concentration from 0.055M to 0.075M [49].

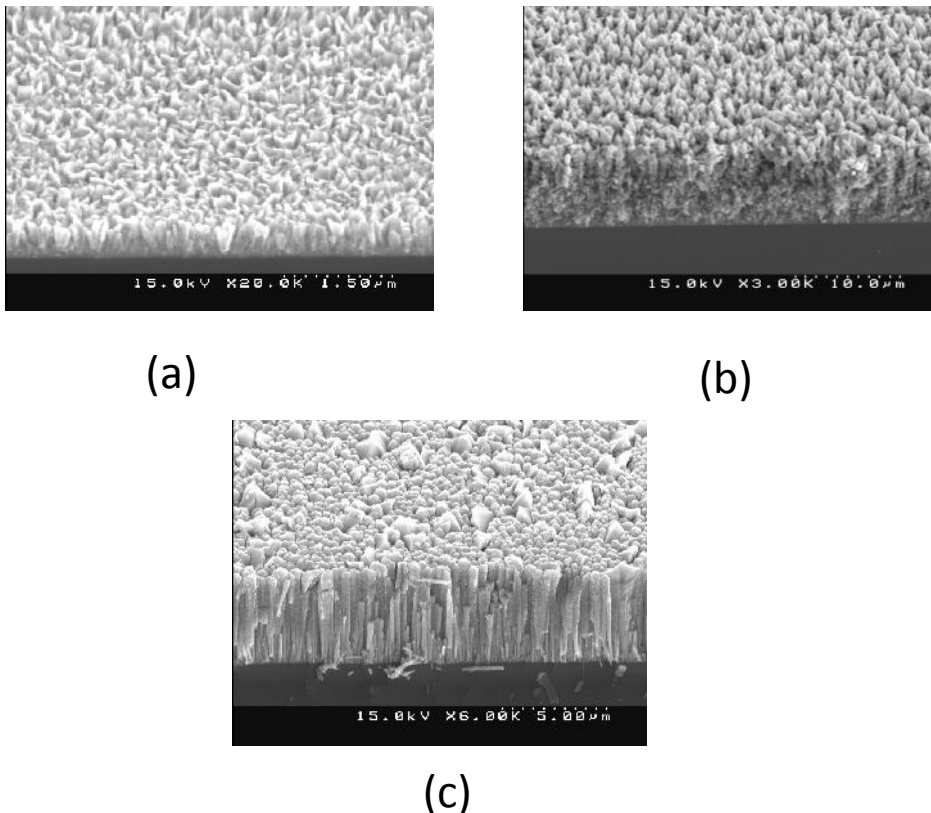


Figure.5.2.1. FE-SEM images of the 1D ZnO nanostructures synthesized in aqueous solution with various molar concentration and temperature. (a) 0.055M at 60°C (b) 0.075M at 80°C (c) 0.055M at 80°C

### 5.3. Fourier Transformed Infrared Spectroscopy (FTIR)

The effective synthesis of ZnO nanostructures from the oxidation of Zn was also confirmed by FTIR analyses, and the spectra are shown in Figure.5.3.1. All oxidised samples present an absorption band ranges from 440-600 $\text{cm}^{-1}$ , related to the stretching mode of Zn-O [50]. The absorption bands at 1108 and 1524 $\text{cm}^{-1}$ , representing atmospheric C-O and C=O adsorbed onto sample. The presence of absorption bands between 1000 and 750 $\text{cm}^{-1}$  in Figure.5.3.1.suggests that sample contained some impurities. The FTIR spectra results are in agreement with the ZnO contents obtained with the X-ray diffraction results. In addition, all spectra showed a band of different shapes and intensities between 3700 and 3200 $\text{cm}^{-1}$ , which is recognized as the O-H stretching mode[50].

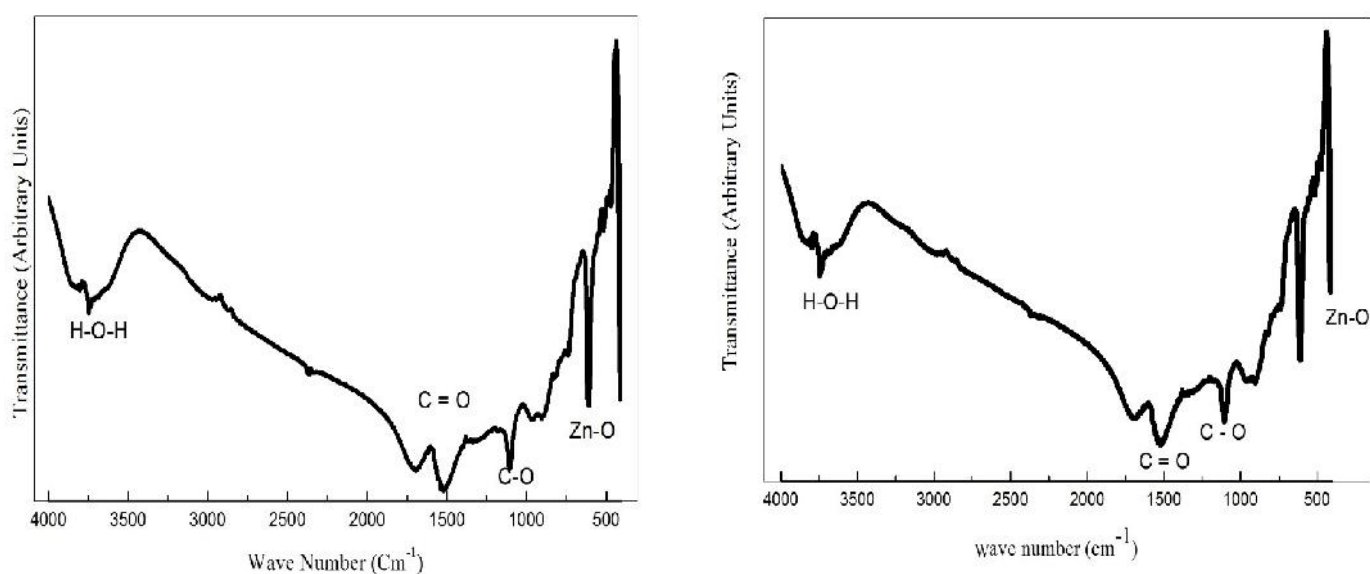


Figure.5.3.1. shows FTIR spectra of ZnO nanostructures synthesized at (a)80°C having concentration 0.055M(b)80°C having concentration 0.075M

## 5.4. Current Voltage (I-V) Measurement

The UV detection characteristics of the ZnO/Si nanostructures were studied by measuring current-voltage I-V relationships with and without UV-B light (310-370) nm. Figure 5.4.1 (a,b). Two cases were studied for the I-V characteristics, one with coating the specimen surface by PSS (Poly Styrene Sulfonate) and other without coating. The linearity of the curve shows the Ohmic contact formed between the metal and semiconductor. The metal contact was formed by coating aluminium on the semiconducting ZnO. For both the cases, current increase rapidly with UV illumination in comparison to dark.

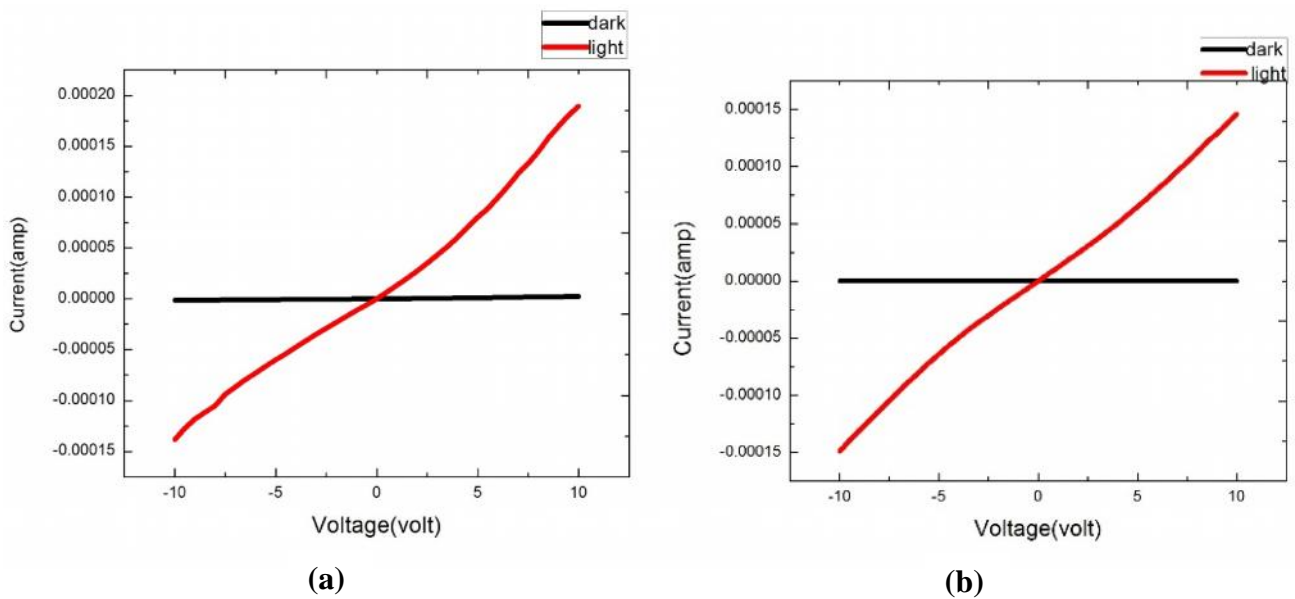


Figure 5.4.1. shows the I-V characteristics of ZnO/Si nanorod before and after UV illumination of (a) Uncoated (b) PSS Coated

## 5.5. UV Detection

Fig. 5.4.2 shows the time evolution of current of the nanorod under UV illumination for surface with modification by coating PSS (Poly Styrene Sulfonate).

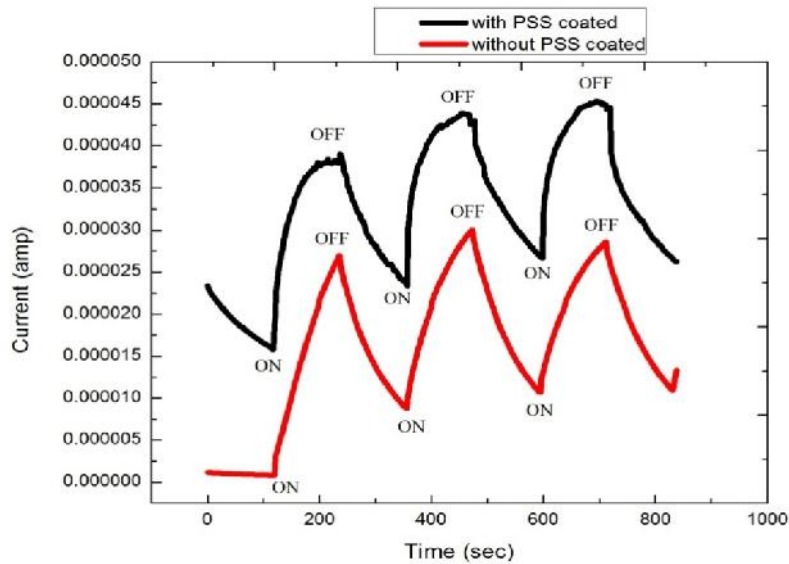


Fig.5.5.1. shows the time evolved photoresponse of the nanorod with PSS coating and without coating

Under UV illumination current increases to a certain value and then decreases for the nanorod without coating with PSS. But for nanorod coated with PSS shows the increase of current to a certain value and then get saturated. After tuning off UV, current comes back to its initial state exponentially. In dark (without UV) the surface of the nanorod acts as preferential site for oxygen adsorption which acts as a potential well for the electron to trap there making a depletion region[51]. So, the photocurrent decreases in dark (without UV). When energy of the incident photon is greater than band gap more number of electron hole pair is generated at the surface. These holes recombine with the adsorbed oxygen ion and decreases the depletion layer and the free electrons increases the current[51]. In case of coating with PSS the value of current saturates due to the higher relaxation time. From the graph it has been found that  $I_{on}/I_{off}$  for the without coating was 0.4013 where as  $I_{on}/I_{off}$  for the nanorods coated with PSS was found to be 0.4405. Thus the increase in  $I_{on}/I_{off}$  value shows better sensitivity of the nanorod coated with PSS due to surface modification.

## **CHAPTER-6**

### **Conclusion**

Zinc Oxide nanostructures were synthesized successfully by local heating method at various concentration and temperature. Crystalline nature of ZnO nanostructures was confirmed by the appearance of high intensity peak at (0 0 2) in X-ray diffraction analysis of different samples. FESEM analysis confirms the formation of long 1D ZnO nanostructures of about 4.5 $\mu$ m in length. The effective synthesis of ZnO nanostructures from the oxidation of Zn was also confirmed by FTIR analyses. The UV detection characteristics of the ZnO/Si nanostructures were studied by measuring current-voltage I-V relationships with and without UV-B light (310-370) nm. UV detection and the corresponding photo response behaviour were studied. Time evolution of current of the nanorods was studied under UV illumination for surface with modification by coating PSS.

## REFERENCES:

- [1] Anderson Janotti and Chris G Van de Walle, Rep. Prog. Phys. 72 (2009) 126501 (29pp)
- [2] D.C. Look, Materials Science and Engineering B80 (2001) 383–387
- [3] Choi Y-S, Kang J-W, Hwang D-K , Park S-J. Recent advances in ZnO-based light emitting diodes, IEEE Trans. Electr. Dev. 2010; 57,26-41.
- [4] P. Yang, H. Yan, S. Mao, R. Russo, J. Johnson, R. Saykally, N. Morris, J. Pham, R. He, H.-J. Choi, Adv. Mater. 12, 323 (2002)
- [5] Zhong Lin Wang, Rev. Phys. Chem., 55 (2004) 96-159
- [6] B. K. Meyer, H. Alves, D. M. Hofmann, W. Kriegseiset al.,Phys. Stat. Sol.,241(2004)231-260.
- [7] M. Risti et al., Journal of Alloys and Compounds, 397 (2005) L1–L4.
- [8]C. Jagadish and S. J. Pearton, “Zinc Oxide Bulk, Thin Films and Nanostructures Processing, Properties and Application” Elsevier (2006).
- [9]Thin-Film Optical Filters, Third Edition By H.A. Macleod
- [10] Material Science of thin films, Milton Ohring
- [11]Nanorods Edited by OrhanYalçın
- [12]Huang et al., 2001b; Giri et al., 2010; Li et al., 2008; Yao et al., 2002
- [13] Yuan & Zhang, 2004; Park et al., 2002; Kim et al., 2009
- [14]Heo et al., 2002
- [15] Breedon et al., 2009; Verges et al., 1990; Alvi et al., 2010;
- [16] Tak Yong, 2005; Pacholski et al., 2002; Song &Lim, 2007
- [17] M.H. Huang, S. Mao, H. Feick, H. Yan, Y. Wu, H. Kind, E. Weber, R. Russo, P. Yang Science, 292 (2001), pp. 1897–1899
- [18] E. W. Petersen, E. M. Likovich, K. J. Russell, and V. Narayanamurti, “Growth of ZnO nanowires catalyzed by size-dependent melting of Au nanoparticles,” Nanotechnology, vol. 20, no. 40, Article ID 405603, 2009
- [19] S. Ashraf, A. C. Jones, J. Bacsá et al., “MOCVD of vertically aligned ZnO nanowires using bidentate ether adducts of dimethylzinc,” Chemical Vapor Deposition, vol. 17, no. 1–3, pp. 45–53, 2011.

- [20] B. Zhang, S. Zhou, B. Liu, H. Gong, and X. Zhang, "Fabrication and green emission of ZnO nanowire arrays," *Science in China, Series E*, vol. 52, no. 4, pp. 883–887, 2009
- [21] Yangyang Zhang, Manoj K. Ram, Elias K. Stefanakos, and D. Yogi Goswami, *Journal of Nanomaterials*, Volume 2012 (2012), Article ID 624520, 22 pages
- [22] B. Liu and H. C. Zeng, "Hydrothermal synthesis of ZnO nanorods in the diameter regime of 50 nm," *Journal of the American Chemical Society*, vol. 125, no. 15, pp. 4430–4431, 2003.
- [23] G. An, Z. Sun, Y. Zhang et al., "CO<sub>2</sub>-mediated synthesis of ZnO nanorods and their application in sensing ethanol vapor," *Journal of Nanoscience and Nanotechnology*, vol. 11, pp. 1252–1258, 2011.
- [24] K. Byrappa and M. Yoshimura, *Handbook of hydrothermal technology*, Elsevier, Oxford, UK, 2013.
- [25] S. Baruah, M. Abbas, M. Myint, T. Bora, and J. Dutta, "Enhanced visible light photocatalysis through fast crystallization of zinc oxide nanorods," *Beilstein Journal of Nanotechnology*, vol. 1, pp. 14–20, 2010.
- [26] F. Xu, Z.-Y. Yuan, G.-H. Du, T.-Z. Ren, C. Volcke, Paul Thiry, B.-L. Su *Journal of Non-Crystalline Solids* 352 (2006) 2569–2574
- [27] T. K. Shing, H. H. Pan, I.-C. Chen and C. I. Kuo, *Tamkang Journal of Science and Engineering*, Vol. 7, No 3, pp. 135138 (2004)
- [28] Liang-Wen Ji, Shi-Ming Peng, Jun-Sheng Wu, Wei-Shun Shih, Cheng-Zhi Wu, I-Tseng Tang, *Journal of Physics and Chemistry of Solids* 70 (2009) 1359–1362
- [29] J.P. Kar, S.W. Lee, W. Lee, J.M. Myoung, *Applied Surface Science* 254 (2008) 6677–6682
- [30] Jin-Bock Lee, Chang-Kyun Park and Jin-Seok Par, *Journal of the Korean Physical Society*, Vol. 50, No. 4, April 2007, pp. 1073~1078
- [31] Naisen Yu, *Appl Phys A* DOI 10.1007/s00339-013-7845-6
- [32] Jyoti Prakash Kar, *Journal of Nanoscience and Nanotechnology*, Vol.10, 1–6, 2010
- [33] J. Kim and I. Park, 14th International Conference on Miniaturized Systems for Chemistry and Life Sciences 3 - 7 October 2010
- [34] Jung Kim et al., *The Royal Society of Chemistry* 2011
- [35] Zheng J. Chew, Lijie Li, *Materials Letters* 76 (2012) 226–228

- [36] D. Kim et al. 978-1-4577-0156-6/2011 IEEE
- [37] C. C. Chen et al. NanoLett. 2011, 11, 4736–4741
- [38] Lulu Chen et al. Journal of Alloys and Compounds 586 (2014) 766–772
- [39] Liang-Yih Chen and Yu-Tung Yin, American Chemical Society, 2012
- [40] J.P. Kar et al., Applied Surface Science 254 (2008) 6677–6682
- [41] Sheng Xu and Zhong Lin Wang , Nano Res DOI 10.1007/s12274-011-0160-7
- [42] Chang Shi Lao et al. J. AM. CHEM. SOC. 2007, 129, 12096-12097
- [43] X-Ray diffraction, B.D. Culity
- [44] Electron Microscopy and analysis, Humphrey and Goodhew
- [45] Fourier Transform Infrared Spectrometry, Peter R. Griffith and James A .De Haseth
- [46] O. Lupan,G. Chai, L. Chow, G. A. Emelchenko, H. Heinrich,V. V. Ursaki, Willey Inter Science, Phys. Status Solidi A, 1–6 (2010) / DOI 10.1002/pssa.200983706
- [47]C. Soci,A. Zhang,B. Xiang, S. A. Dayeh, D. P. R. Aplin, J. Park, X. Y. Bao, Y. H. Lo, and D. Wang,Nano letters 2007,Vol.7 No- 4 1003-1009
- [48] F. Fang, Science direct, Materials Letters 62 (2008) 1092–1095
- [49] J. P. Kar et al. Surface Modification of Hydrothermally Grown ZnO, DOI: 10.1080/00986440902897491, Chem. Eng. Comm., 196:1130–1138, 2009
- [50] Y. J. Kwon, K. H. Kim, C. S. Lim and K. B. Shim,“Characterization of ZnONanopowders Synthesized by the Polymerized Complex Method via an Organ chemical Route,” Journal of Ceramic Processing Research, Vol. 3, No. 3, 2002, pp. 146-149.
- [51] J.P. Kar et al. / Journal of Crystal Growth 311 (2009) 3305–3309